Multiband Triple L-Arms Patch Antenna with Diamond Slot Ground for 5G Applications

Dalia H. Sadek [1], Heba A. Shawkey [2], and Abdelhalim A. Zekry [1]

[1] Faculty of Engineering, Ain Shams University, Cairo, Egypt
Doly_sadek@hotmail.com, aaazekry@hotmail.com

[2] Electronics Research Institute (ERI) Giza – Egypt
heba_shawkey@eri.sci.eg

Abstract ─ This paper reported a pioneering 5G multiband microstrip line fed patch antenna for IoT, wireless power transfer (WPT) and data transmission. The proposed antenna is accomplished using a triple L-arms patch antenna responsible for the multiband response. A diamond-shaped ground slot is added to control and increase the bandwidth of the resonant frequency. The antenna is designed to resonate at 10, 13, 17 and 26 GHz with 10 dB impedance bandwidths of 0.67, 0.8, 2.45 and 4.3 GHz respectively. The proposed antenna is fabricated using microstrip technology with total area of 16.5x16.5 mm^2. The 5G multiband antenna has sufficient realized gain of 4.95, 5.72, 4.94 and 7.077 dB respectively. The antenna is designed and simulated using the CST Microwave Studio Suite (Computer Simulation Technology). Measurements show good agreement with simulations in all frequencies of operation.

Index Terms ─ 5G wireless communication, diamond-shaped slot, Internet of Things (IoT), Millimeter Wave (MMW), multiband antenna, Triple-L Arms (TLA), Global System for Mobile Communications (GSM).

I. INTRODUCTION

The demand for the high data rate transfer and large capacities of traffic is continuously growing so, the world will witness 5G technology very soon with the fastest broadband speed and low latency. It needs to operate in three frequency ranges to ensure widespread coverage and support for all networks covered by previous technology. These ranges are Sub-1GHz, 1–6 GHz and above 6 GHz [1]. With a strength of sub-1GHz, it cannot meet the requirements in terms of absolute high bandwidth. It is used to provide broad coverage in urban areas and suburbs. The 1–6 GHz band provide both capacity and coverage advantages. The band above 6 GHz fulfills the requirements of an ultra-high broadband speed of 5G. There would be a need to use MMW bands starting from 24 GHz to satisfy the need for high broadband speeds up to 20 Gb/s [2]. GSM has proposed mobile bands of 26 GHz (24.25 GHz-27.5 GHz), 40 GHz (37.5 GHz-43.5 GHz) and (67 GHz-71 GHz) [3],[4]. The infrastructure for 5G mobile channels will be able to support much better data speeds, higher aggregate capacity, minimal latency, lower infrastructure cost, and many new capabilities due to increased bandwidth [5]. Antenna for 5G communications should consider some key requirements of 5G technology. It should resonate over a wide bandwidth, continuous strong connections with minimum latency. Multiband antenna is a potential solution for battery-less wireless applications that need multiple channels for simultaneous data and power transfer as wearable/implantable medical devices, smart farming sensors and portable electronics devices [6]–[8].

There are many proposed antennas for 5G bands with different applications. For example, Yahia et al. have designed a compact directional microstrip grid array antenna at 10 GHz. The antenna was designed on a cheap FR4 substrate and has achieved a dual band with peak gain of 8.03 dBi [9]. For wireless power transfer and harvesting applications, there are appropriate choices of frequency to ensure high RF-DC power conversion. In [10], Abderrahim et al. designed multiband rectenna for microwave applications. The antenna can harvest ambient power at different radio frequencies of 12, 17, and 20 GHz. Some studies have been done at 26 and 28 GHz [11] by Mahmoud et al. The antenna has been fabricated using standard commercial materials, to produce MMW antenna on textile for radio frequency energy harvesting (RFEH), enabling high efficiency reception of MMW radiation for wearable rectennas. In [12], Farzad et al. designed broadband circularly polarized array antenna using FR4 substrate with a thickness of 0.8 mm. It designed with an L-shaped patch and a rhombic slot in the ground. This antenna can cover the frequency band 4.66–5.30 GHz. In [13], the Varum et al. introduced a microstrip antenna for IoT which resonates at band 17 GHz with More than 2 GHz bandwidth and gain 5.8 dBi. In [14], Ebenezer et al. designed a compact ultra-light weight and efficient

Submitted On: October 11, 2020
Accepted On: February 8, 2021

https://doi.org/10.47037/2020.ACES.J.360310

circularly polarized asymmetric slit patch antenna. It is fabricated using RT/DUROID 5880 material to operate at the center frequency of 11.3 GHz and constant gain through the operating bandwidth with an apprehended peak gain of 5.6 db for vehicular satellite communication applications. In this work, a multiband microstrip antenna was designed to achieve a high gain with small size at 5G bands of 10, 13, 17 and 26 GHz. The antenna is small enough to be included in sensors, domestic equipment's and wearables. Also, it is appropriate for WPT and energy harvesting systems, the multiband operation increases the harvesting power compared with single band operation, where the receiving antenna collects the power from multiband. The designed antenna has the advantages of structural simplicity, planar geometry, ease of fabrication and relatively lower complexity. This paper is comprised of four sections. Section 2 includes the design and layout of the presented antenna, Section 3 contains the implementation and measurement while the last section concludes the paper.

II. ANTENNA DESIGN AND LAYOUT

The structure geometry of the proposed Triple – L arms patch slotted antenna (TLA) is shown in Fig. 1. The antenna is designed using ROGERS(RO4003c) substrate with relative dielectric permittivity ε_r=3.38, thickness 0.81 mm and dissipation factor tanδ=0.0026. The feeding line with width of W_f =2.1mm and length of L_f =6.3 mm to feed the antenna.

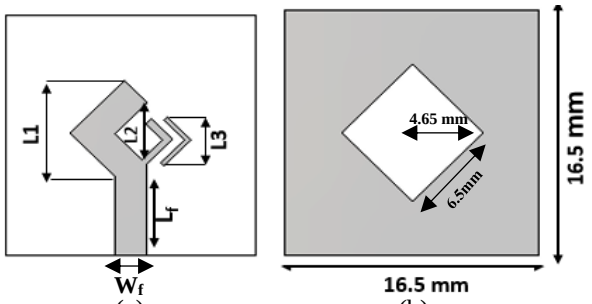

(a) (b)

Fig. 1. Configuration of the proposed antenna with dimensions: (a) top view and (b) bottom view.

The design consists of a slotted antenna having a microstrip feed line and three L-shaped arms, each responsible for a certain resonant frequency. To improve resonant frequencies' bandwidth, a diamond slot shown in Fig. 1 (b), has been carved on the opposite side of the radiation patch on the ground plane of the antenna at a distance of 4.65 mm from the center of the ground with length 6. 5mm.The key design is to set the length of each arm close to the half wavelength of the resonant frequency (L~λ/2). L_1~ 15mm, L_2~5.7mm, L_3~8.8mm. Because of the existence of an electromagnetic coupling between the 3 arms, a parametric study has been carried out to define the optimum length for the required frequency bands.

Design flow was done in 3 steps. In the first step, only one arm patch L_1 is set with its dimensions are adjusted to (5.9mm,4.83mm) to generate the 10 GHz resonant frequency. To get the second band another arm L_2 with length of (2.5mm,2.9mm) has been added to get resonant at 26 GHz. Finally, the arm L_3 with length of (3mm,3.4mm) generates a resonant at 17 GHz. Figure 2 illustrates simulation results for the 3 design steps of the TLA antenna with diamond slot ground. The length of the feed line is made 4.6 mm, and its width is made 2.1 mm in order to match the impedance of the patch. To optimize operation bandwidth of the proposed antenna, the dimensions of the diamond slot ground are changed. Figure 3 indicates a comparison of S11 parameter for the proposed antenna with different slot size .The figure clarifies that the bandwidth of resonant frequencies can be adjusted by changing the values of ground slot to reach a wider bandwidth specially at the higher bands of resonant frequencies which is suitable to WPT and harvesting systems application. The wide bandwidth aims to solve traffic-related issues. And the wide bandwidth antennas are necessary to harvest power efficiently from the full spectrum.

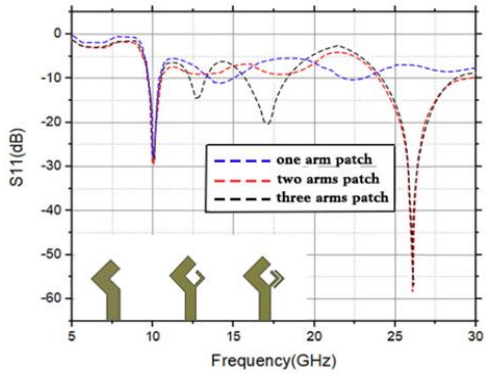

Fig. 2. The reflection coefficient of the design steps for the proposed antenna.

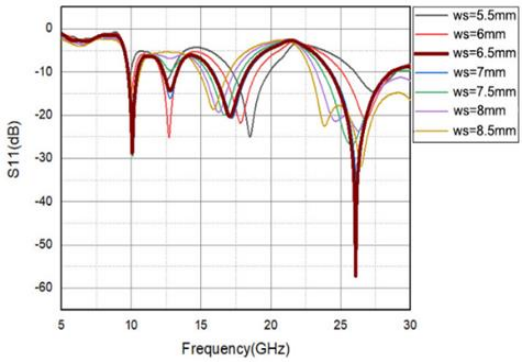

Fig. 3. Adjustment in the bandwidth of the antenna for different values of ground slots.

III. ANTENNA IMPLEMENTATION AND MEASUREMENT

The TLA antenna fabricated using Photolithography technology with wet etching and the track's pattern plotted on a dark-film mask in Microstrip Fabrication Laboratory, Electronics Research Institute (ERI). Figure 4 shows a photograph for the fabricated TLA. Figure 5 clarifies the test feature to connect the proposed antenna with vector network analyzer (VNA). Figure 6 shows the VNA (ROHDE&SCHWARZ ZVA6) that it is used to perform the return loss measurements.

A. Designed antenna S-parameters

Figure 7 depicts the simulated in addition to measured results of the proposed antenna for sake of validation and comparison. The antenna was initially simulated and optimized for 10, 17 and 26 GHz, but the simulation shows an extra resonant frequency at 13 GHz this can be explained due to the effect of the ground slot. It is clear that the antenna has sufficient bandwidth at the resonant frequencies. 10 GHz band has bandwidth of 0.67 GHz with minimum return loss of 28.17 dB,13 GHz band with 0.8GHz bandwidth and 15dB minimum return loss, 17GHz band has a bandwidth of 2.45 GHz with minimum return loss of 20.327 dB and 26 GHz band has bandwidth of 4.3 GHz with minimum return loss of 57.15dB, where the bandwidth is determined at -10dB reflection coefficient level as a reference. It is clear from Fig. 7 that there is good agreement at the lower frequencies while there is an appreciable loss at the higher frequency side of the S11 curve This is due to the additional parasitic capacitance in experimental device in addition to the effects of the connectors at such higher frequencies. Moreover, there are also fabrication tolerances [17].

B. Equivalent circuit of the TLA antenna (modeling of patch antenna)

This section describes the electrical equivalent circuit of the TLA antenna Fig. 8 (a) shows the equivalent circuit used to model the electrical behavior of the antenna in response to an incoming RF input signal. It is particularly useful to implement this model using basic components R1, L1, and C1, which influence the first resonant frequency ($f1$), R2, L2, and C2 influence the second resonant frequency ($f2$), R3, L3, and C3 influence the third resonant frequency ($f3$) and finally, R4, L4, and C4 influence the fourth resonant frequency ($f4$). Elements L5 and C5 are included in the equivalent circuit model to represent the electrical length of the feed line and the slot coupling, respectively. The corresponding values of the equivalent circuit elements are depicted in Table 1. Figure 8 (b) shows the reflection coefficient response of the antenna obtained from CST simulation compared to the calculated response of the equivalent circuit model by using Agilent ADS software in addition to the measured reflection coefficient. The results of simulated, measured, and ADS model are in good agreement.

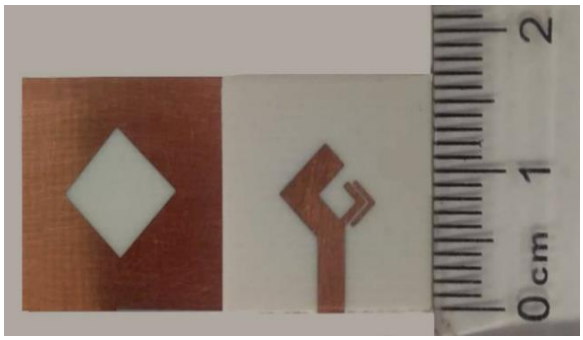

(a) (b)

Fig. 4. Photograph of the fabricated patch antenna: (a) bottom layer and (b) top layer.

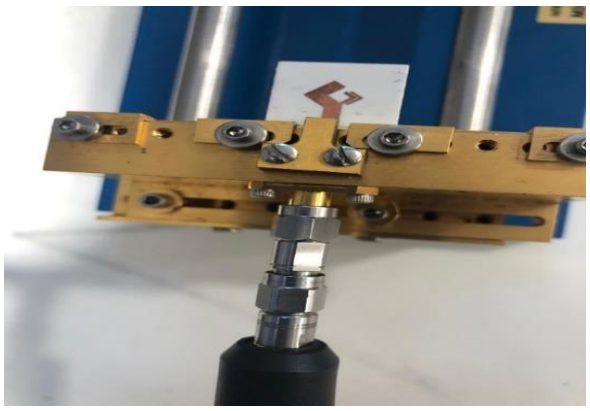

Fig. 5. Microwave test feature to connect the antenna with Vector Network Analyzer.

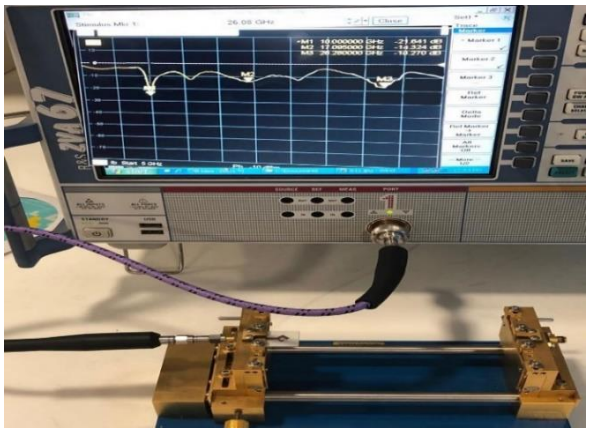

Fig. 6. The measurement of S11 parameter using the VNA ROHDE&SCHWARZ ZVA6.

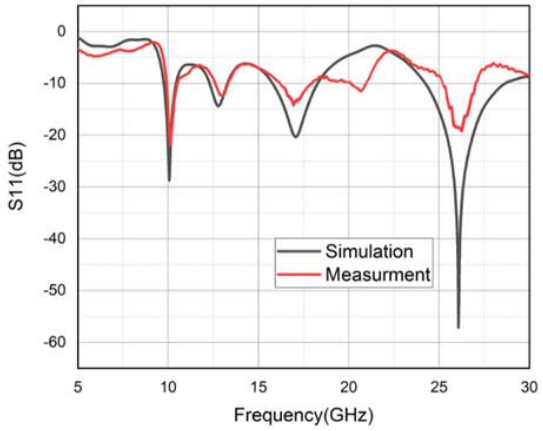

Fig. 7. Comparison between simulation and measured reflection coefficient versus frequency.

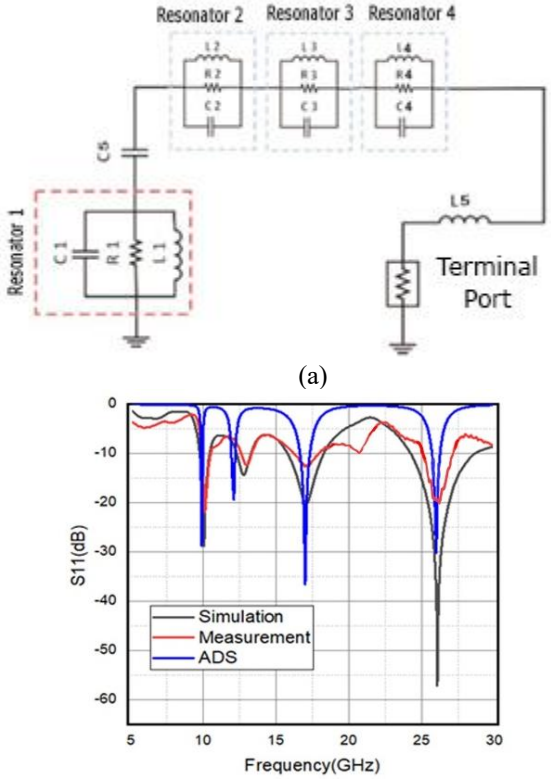

Fig. 8. (a) Equivalent lumped-elements circuit for antenna in ADS. (b) Comparison of the reflection coefficient responses of CST, ADS and measurement.

C. Surface current distribution

Figures 9 (a), (b), (c) and (d) describes the current distribution of the TLA antenna at frequency bands 10, 13, 17 and 26 GHz, respectively. It is observed from these figures that the currents are concentrated at the outer edges of radiating patches. Also indicates that each arm is responsible for a specific resonant frequency [18]. This means that the largest arm gives 10 GHz resonant and the smallest arm gives 26 GHz resonant, as mentioned before in the design antenna procedure. The current distribution on the antenna at 13 GHz indicates that the ground slot is responsible for this resonant frequency.

D. 2D-Polar radiation patterns

The radiation pattern comparison measured and simulated of the antenna at 10 and 13 GHz are depicted in Figs. 10 (a) and (b). The solid red and black line represents the simulated E-plane and H-plane respectively. Also, the dashed red and black line represents the measured E-plane and H-plane. The pattern depicts a dipole-like pattern in both measured and simulated results. The simulated radiation patterns at operating bands 17 and 26 GHz frequencies shown in Figs. 10 (c) and (d). The solid red and black line represents the simulated E-plane and H-plane. Measurements were only made for frequencies 10 and 13GHz due to the instrumentation capabilities available at the ERI lab. It can be observed that the slot in the ground plane influences the patterns in the backward direction at the resonant frequencies. This is because the slot in the ground plane is itself resonators. Also, it can be notice that at the higher frequency (26 GHz) the radiation pattern deteriorates because of unequal phase distribution and significant magnitude of higher order modes. For a further completing the antenna performance, plot of antenna's gain is presented in Fig. 11. The plot illustrates that antenna has a relatively high gain at frequencies 10,13,17 and 26 GHz of 4.95, 5.72, 4.94 and 7.077 dB respectively. which is a good gain compared to the antenna introduced by the author in [11] that provides a gain of 5.4 dB in space at 26 GHz. Also, with total efficiency of 90%, 94.6%, 92% and 93.3% respectively.

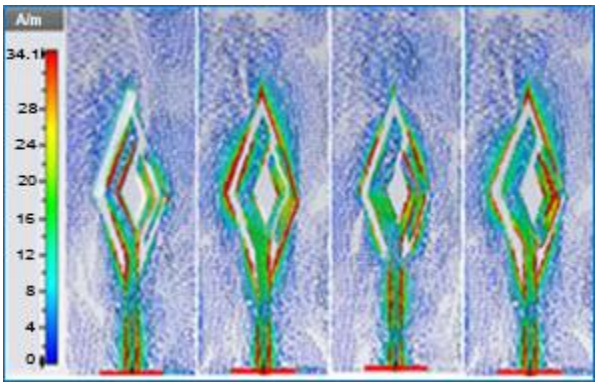

Fig. 9. Current distribution of 5G antenna at the resonant frequencies (a) 10 GHz (b) 13 GHz (c) 17 GHz (d) 26 GHz.

Table 1: Elements values of the equivalent circuit model

Parameter	R1 (Ω)	L1 (nH)	C1 (pF)	R2 (Ω)	L2 (nH)	C2 (pF)	R3 (Ω)	L3 (nH)	C3 (pF)	R4 (Ω)	L4 (nH)	C4 (pF)	L5 (nH)	C5 (pF)
Value	383	0.1	3.5	340	.14	1.3	332	0.2	.47	516	0.1	0.4	1.1	10

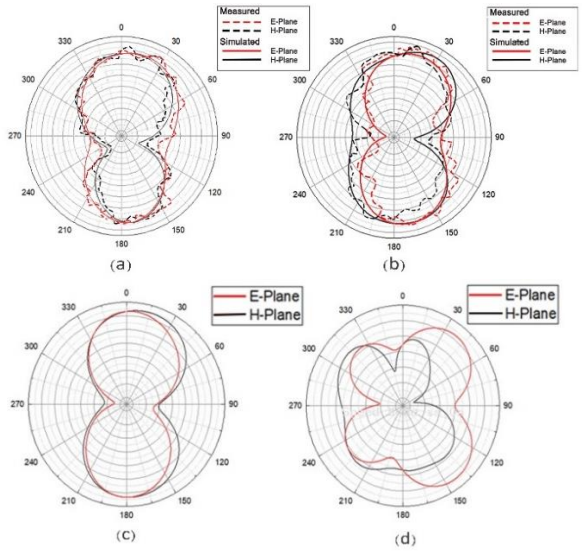

Fig. 10. The radiation pattern of the proposed antenna in E-plane and H-plane.

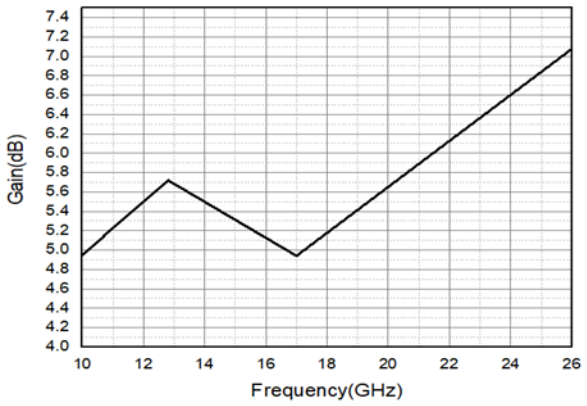

Fig. 11. Gain versus frequency.

Table 2 shows the performance comparison between the TLA antenna and other previously reported in literature within the same frequency range. Compared with other types, the TLA antenna has large number of resonant frequencies, except for [10] the TLA antenna has one more band with smaller area. Besides it operates in the low frequencies 10 and 13 GHz with no area overhead compared with other types operate in comparable frequency band. The proposed antenna has larger gain at 26 GHz compared with that antenna presented in [11] but the antenna uses a commercial textile material for wearable ambient RFEH. While in [12] and [13] a single band of operation, for [12] with one arm patch, larger area and lower gain and for [13] with smaller area and higher gain compared to the proposed antenna. In [15], multiband antenna with lower frequencies and larger area but with larger bandwidth compared with the lower frequency of the TLA antenna. The area of antenna designed in [16] is smaller than the proposed antenna but with less bandwidth such area is compatible to be a unit of an array.

Table 2: Comparison of the proposed antenna with other antennas

Reference	Operating frequency (GHz)	BW (GHz)	S11 dB	Gain (dBi)	Antenna size (mm^2)
[9]	10-10.68/ 10.7-12.23	0.65-1.5	16.33/ 31.9	8.03	48x55
[10]	12/17/20	--------	35/14/ 16	11.7/ 11.7/ 17.6	19.5x19.5
[11]	26/28	--------	18/21	5.4/5.5	30x55
[12]	4.95	0.64	30	3.39	32 x 46
[13]	17	2.2	---------	5.8	4x4
[15]	5.2/5.4/5.8	1.3	~14	6.5	50x50
[16]	26/28	2.28	>12	---------	6x6
This work	10/13/17/ 26	0.67/ 0.8/ 2.45/ 4.3	28/15/ 20/57	4.95/ 5.72/ 4.94 / 7.077	16.5x16.5

IV. CONCLUSION

A slotted microstrip patch antenna having four resonant modes for use in IoT, WPT and data transmission. has been proposed and studied.

The antenna is a very low-profile structure with dimensions 16.5×16.5×0.81mm^3. It can hence, be easily integrated into devices with space constraints. The TLA antenna is designed to operate at 10, 13, 17 and 26 GHz with a bandwidth of 0.67, 0.8, 2.45 and 4.3 GHz, respectively. The wide bandwidth antennas are necessary to harvest power efficiently from the full spectrum. The maximum efficiency is achieved at 13 and 26 GHz. The antenna was fabricated and measured with a good agreement between the simulation results and measurement results for reflection coefficient in addition to radiation characteristics.

REFERENCES

[1] A. Morgado, K. M. Huq, S. Mumtaz, and J. Rodriguez, "A survey of 5g technologies: Regulatory, standardization and industrial perspectives," *Digital Communications and Networks*, vol. 4, no. 2, pp. 87-97, 2018.

[2] T. S. Rappaport, R. W. Heath, Jr., R. C. Daniels, and J. N. Murdock, *Millimeter Wave Wireless*

Communications. Pearson Education, 2014.

[3] T. S. Rappaport, Y. Xing, G. R. Mac Cartney, Jr., A. F. Molisch, E. Mellios, and J. Zhang, "Overview of millimeter wave communications for fifth-generation (5g) wireless networks-with a focus on propagation models," arXiv preprint arXiv:1708. 02557, 2017.

[4] Y. Niu, Y. Li, D. Jin, L. Su, and A. V. Vasilakos, "A survey of millimeter wave communications (mmwave) for 5g: Opportunities and challenges," *Wireless Networks*, vol. 21, no. 8, pp. 2657-2676, 2015.

[5] C. X. Wang, F. Haideret, X. Gao, Y. Xiaohu, Y. Yang, D. Yuan, H. M. Aggoune, H. Haas, S. Fletcher, and E. Hepsaydir, "Cellular architecture and key technologies for 5G wireless communication networks," *IEEE Communication Mag*., vol. 52, no. 2, pp. 122-130, Feb. 2014.

[6] H. Shawkey and D. Elsheakh, "Multiband dual-meander lie antenna for body-centric networks' biomedical applications by using UMC 180 nm," *Electronics MDPI Journal*, 2020.

[7] Q. Bai, R. Singh, K. L. Ford, T. O. Farrell, and R. J. Langley, "An independently tunable tri-band antenna design for concurrent multiband single chain radio receivers," *IEEE Transactions on Antennas and Propagation*, vol. 65, no. 12, Dec. 2017.

[8] D. Zhai, R. Zhang, J. Du, Z. Ding, and F. R. Yu, "Simultaneous wireless information and power transfer at 5G new frequencies: Channel measurement and network design," *IEEE Journal on Selected Areas in Communications*, 2018.

[9] M. S. Yahya, I. A Dalyop, Y. Saleh, and M. Aminu-Baba, "Antenna for 5G mobile communications systems at 10 GHz," in *International Journal of Engineering & Technology*, 7 (3.36), pp. 13-15, 2018.

[10] A. Okba, A. Takacs, H. Aubert, S. Charlot, and P. F. Calmon, "Multiband rectenna for microwave applications," *Elsevier Comptes Rendus Physique*, vol. 18, no. 2, pp. 107-117, Feb. 2017.

[11] M. Wagih, A. S. Weddell, and S. Beeby, "Millimeter-wave textile antenna for on-body RF energy harvesting in future 5G networks," in *Wireless Power Transfer Conference (WPTC), IEEE*, 2019.

[12] F. Zandikiya and L. Asadpor," Broadband circularly polarized slot antenna array fed by asymmetric CPW for C-band applications," *IETE Journal of Research*, 2017.

[13] T. Varum, M. Duarte, J. N. Matos, and P. Pinho, "Microstrip antenna for IoT/WLAN applications in smart homes at 17GHz," *12th European Conference on Antennas and Propagation (EuCAP)*, 2018.

[14] A. B. Ebenezer, A. Raaza, S. Ramesh, S. Jerritta, and V. Rajendran, "Circularly polarized circular slit planar antenna for vehicular satellite applications," *Applied Computational Electromagnetics Society Journal*, vol. 34, no. 9, pp. 1340-1345, Sep. 2019.

[15] M. Simone, A. Fanti, L. Boccia, G. Amendola, and G. Mazzarella, "A dual polarized stacked antenna for 5G mobile devices," *Photonics & Electromagnetics Research Symposium | Spring (PIERS | SPRING)*, 2019.

[16] M. Simone and N. Curreli, "Design of a multiband WLAN antenna," *Loughborough Antennas and Propagation Conference (LAPC). IEEE*, 2014.

[17] G. S. Karthikeya, M. P. Abegaonkar, and S. K. Koul, "Low cost high gain triple band mmwave Sierpinski antenna loaded with uniplanar EBG for 5G applications," *IEEE International Conference on Antenna Innovations & Modern Technologies for Ground, Aircraft and Satellite Applications*, 2017.

[18] P. Bhartia, I. Bahl, R. Garg, and A. Ittipiboon, *Handbook of Microstrip Antennas Design*. Norwood: Artech House, 2001.